*Exploration Geophysics (2004) **35**, 7–13*
Butsuri-Tansa (Vol. 57, No. 1)
Mulli-Tamsa (Vol. 7, No. 1)

CMP cross-correlation analysis of multi-channel surface-wave data

Koichi Hayashi[1] **Haruhiko Suzuki**[2]

Key Words: *surface waves, CMP, cross-correlation*

ABSTRACT

In this paper, we demonstrate that Common Mid-Point (CMP) cross-correlation gathers of multi-channel and multi-shot surface waves give accurate phase-velocity curves, and enable us to reconstruct two-dimensional (2D) velocity structures with high resolution. Data acquisition for CMP cross-correlation analysis is similar to acquisition for a 2D seismic reflection survey. Data processing seems similar to Common Depth-Point (CDP) analysis of 2D seismic reflection survey data, but differs in that the cross-correlation of the original waveform is calculated before making CMP gathers. Data processing in CMP cross-correlation analysis consists of the following four steps: First, cross-correlations are calculated for every pair of traces in each shot gather. Second, correlation traces having a common mid-point are gathered, and those traces that have equal spacing are stacked in the time domain. The resultant cross-correlation gathers resemble shot gathers and are referred to as CMP cross-correlation gathers. Third, a multi-channel analysis is applied to the CMP cross-correlation gathers for calculating phase velocities of surface waves. Finally, a 2D S-wave velocity profile is reconstructed through non-linear least squares inversion. Analyses of waveform data from numerical modelling and field observations indicate that the new method could greatly improve the accuracy and resolution of subsurface S-velocity structure, compared with conventional surface-wave methods.

INTRODUCTION

Delineation of S-wave velocity structure down to the depth of 15 m is very important in engineering and environmental problems. PS-logging has been adopted for this purpose for years. However, PS-logging is not generally convenient for surveying, as it requires a borehole. Drilling a borehole and operating a logging tool are expensive. There have been growing demands for more convenient methods for determining shallow S-wave structures.

It is well known that the dispersion of phase velocity of surface waves (Rayleigh waves) is mainly determined by S-wave velocity structure. The use of surface waves for near-surface S-wave delineation has been the subject of many studies in the past decade. For example, the spectral analysis of surface waves (SASW) has been used for the determination of 1D S-velocity structures down to 100 m (Nazarian et al., 1983). Most of the surface-wave methods described have employed a shaker or a vibrator as sources, and have calculated phase differences between two receivers using a simple cross-correlation technique.

Park et al. (1999a, 1999b) proposed a multi-channel analysis of surface waves (MASW). Their method determines phase velocities directly from multi-channel surface-wave data after applying an integral transformation to the frequency-domain waveform data. The integration directly converts time-domain waveform data (time-distance) into an image of phase velocity versus frequency (c–f). The MASW method is much better than SASW because the MASW method can allow the fundamental mode of Rayleigh wave dispersion to be distinguished visually from other modes, such as higher modes and body waves. In addition to this, the MASW method can avoid spatial aliasing, which is a problem in the SASW method. Xia et al. (1999) and Miller et al. (1999) applied the MASW method to continuous-profiling shot records, and delineated 2D S-wave velocity structures.

In order to determine phase velocities at low frequencies precisely, Park et al. (1999a) pointed out that it is essential for the MASW method to use as long a receiver array as possible. However, a longer receiver array might decrease the lateral resolution of the survey, because the conventional MASW method provides a velocity model averaged over the total length of the array. A smaller array is better for increasing lateral resolution. Improved lateral resolution is traded off against accuracy of phase velocity. We have developed the following method to overcome this trade-off.

COMMON MID-POINT CROSS-CORRELATION

Figure 1a shows an example of multi-channel surface-wave data obtained using an impulsive source. Dispersive later phases can be observed, and their apparent velocities change suddenly at the middle of the spread, indicating a lateral change in velocity structure around the middle point of the spread (Distance = 185 m). Figure 1b shows a c–f image computed by the MASW method. Such a dispersion image, split into two or three curves, indicates no unique phase velocity. The appearance of the dispersion image is similar to that produced from a finite-difference numerical model having a lateral velocity change (Hayashi, 2001).

The MASW method can be considered essentially as a summation of cross-correlations of all wave traces. Dispersion relationships are obtained by using pairs of observation points. Then structures are estimated at the midpoints of the entire array spread used. Figure 2a illustrates a relationship between locations of observation points and estimated velocity structure. The horizontal location where velocity structure is estimated corresponds to the midpoint of the entire array spread. If we wish to improve the resolution of phase velocity, we must use many receiver pairs. However, increasing the correlation distance degrades lateral resolution. Thus, there is a trade-off between the number of correlation pairs and the correlation distance, when improving phase velocity measurement.

[1] *43 Miyukigaoka, Tsukuba, Ibaraki, Japan 305-0841*
Tel: +81-298-51-6621
Fax: +81-298-51-5450
Email: hayashi-kouichi@oyonet.oyo.co.jp

[2] *43 Miyukigaoka, Tsukuba, Ibaraki, Japan 305-0841*
Email: suzuki-haruhiko@oyonet.oyo.co.jp

Manuscript received July 15, 2003; accepted September 19, 2003. Part of this paper was presented at the 6th SEGJ International Symposium (2003).

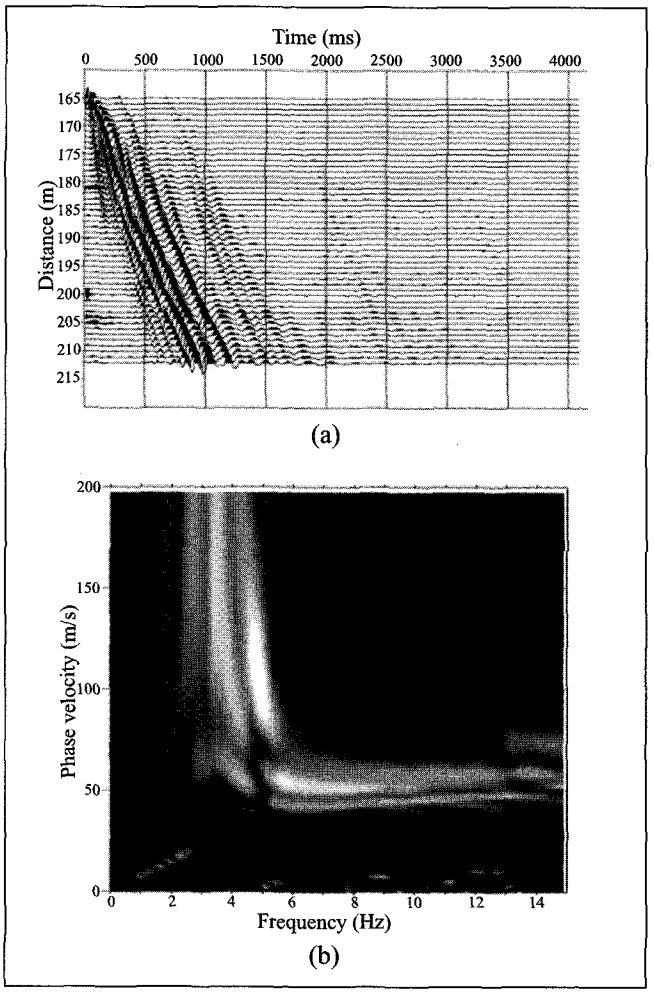

Fig. 1. (a) An example of observed shot records. (b) The *c–f* image of Figure 1a. White indicates largest amplitude.

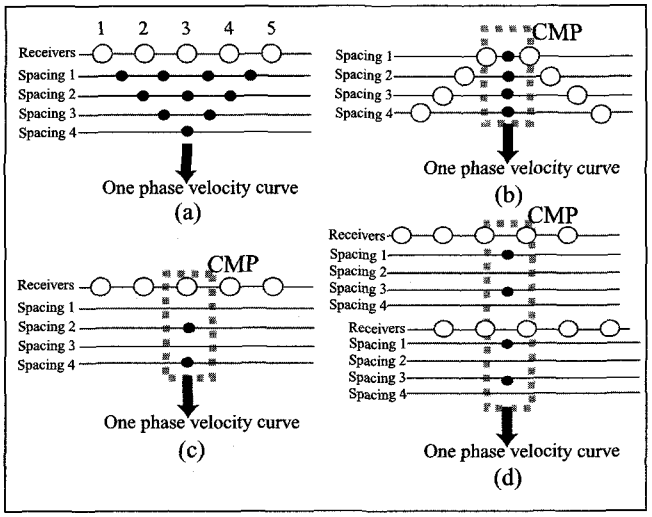

***Fig. 2. The concept of CMP analysis in the surface-wave method.* The open circles indicate receiver locations and the solid circles indicate the midpoints of cross-correlations. Spacing 1, 2, 3, ... refers to the receiver distances for calculating cross-correlation; for example, *spacing 1 corresponds to the pairs* 1–2, 2–3, 3–4, and 4–5, whereas spacing 2 corresponds to the pairs 1–3, 2–4 and 3–5. (a) Location of observation points, and estimated velocity structure, in conventional MASW analysis. (b) Cross-correlation that has same CMP locations (CMPCC). (c) CMPCC for one shot. (d) CMPCC for multiple shots.**

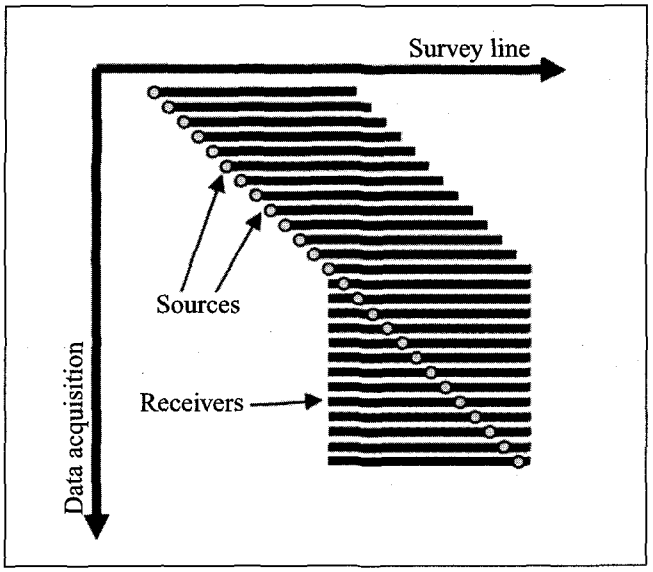

Fig. 3. A source-receiver geometry of moving-source observation of surface waves for CMP analysis.

To improve the lateral resolution, we must use cross-correlations that have the same common-mid-point locations, as shown in Figure 2b. Henceforth, we use the term "CMPCC" to refer to cross-correlations that have a common mid-point. If we use a CMPCC process on a single shot gather, cross-correlations that have different midpoints are thrown away. Take Figure 2a, for example. Ten pairs can be extracted from five traces, but only two traces can be grouped for the CMPCC process. To increase the number of CMPCC data, we use a multi-shot method and move the receiver spread and shot points, as in the reflection seismic method. Then the number of CMPCC points can be increased, as shown in Figure 2d.

Data acquisition for the CMPCC method is similar to acquisition for a 2D seismic reflection survey. Source-receiver geometry is based on the end-on spread, and both source and receivers move up along a survey line. Receivers can be fixed in position at the end of the survey line (Figure 3). CDP cables, and a CDP switch, as used in a 2D seismic reflection survey, enable us to perform data acquisition easily. Ideally, the source and receiver intervals should be identical. However, considering the resolution of surface waves and the efficiency of data acquisition, it is better that the source interval be longer than the receiver interval.

ANALYSIS

The authors have developed the CMPCC analysis to be applied to multi-channel and multi-shot surface-wave data. The procedure for a CMPCC analysis is summarised in the following way:

1. In each shot gather, cross-correlations are calculated for every pair of traces (Figure 4a). For example, 276 cross-correlations (= 24C2) are calculated from a shot gather that includes 24 traces.
2. After cross-correlating every pair of all shot gathers, correlations having a common mid-point are grouped together.
3. At each common mid-point, cross-correlations that have an equal spacing are stacked in the time domain (Figure 4b, c). Even if each source wavelet and its phases are different, cross-correlations can be stacked because the correlation stores only phase differences between two traces. The phase differences contained in the source wavelet have been removed.
4. The cross-correlations that have different spacing should not be stacked in the time domain. These cross-correlations are ordered with respect to their spacing, at each common mid-point (Figure 4d). The resultant cross-correlation gather resembles shot gathers. However, it contains only

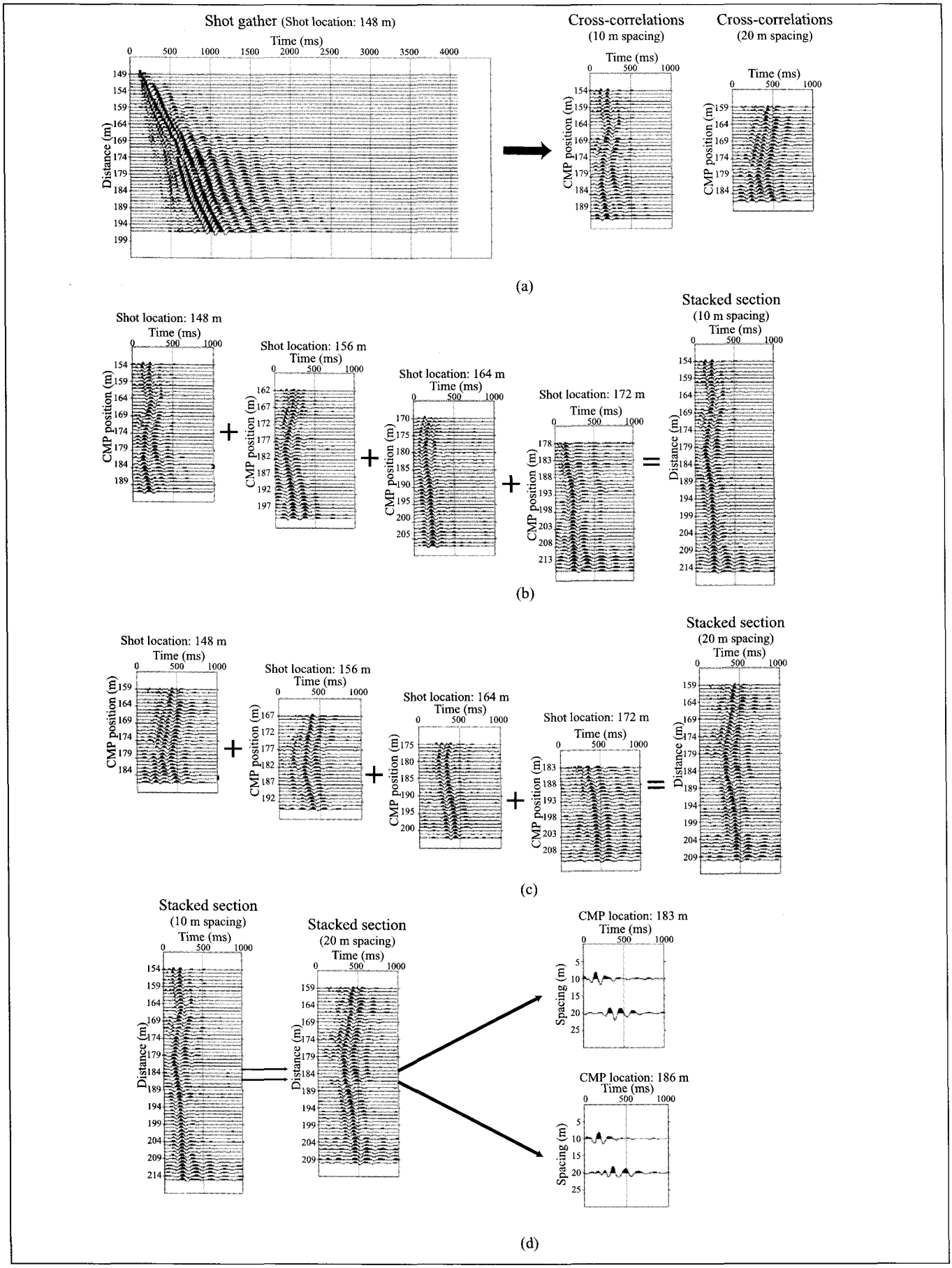

Fig. 4. An example of data processing of CMPCC analysis for four shots. (a) Calculation of cross-correlations from one shot gather (step1). (b) and (c) Time domain stacking of cross-correlations that have identical spacing (step3). (d) Different spacing cross-correlations are ordered with respect to lateral distance. The CMPCC gathers are obtained for each distance. All shot-gathers in the survey line are used, and cross-correlations are calculated for every pair of traces.

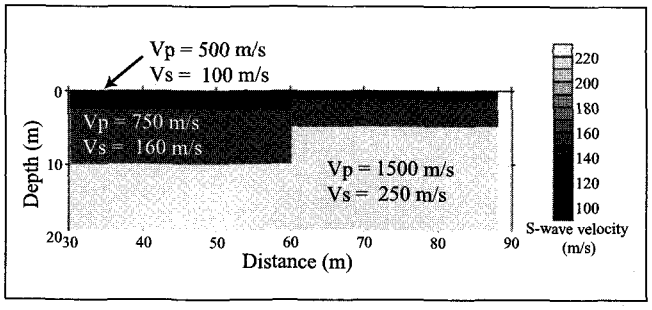

Fig. 5. Velocity model used for the numerical test.

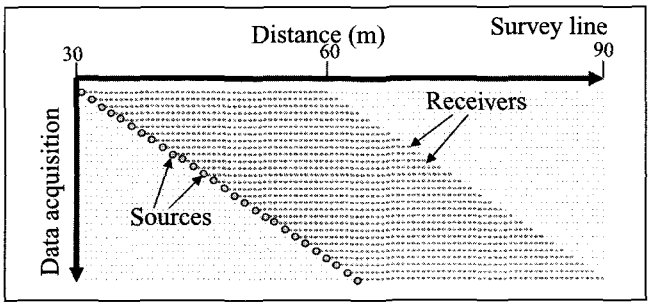

Fig. 6. Source-receiver geometry used in the numerical test.

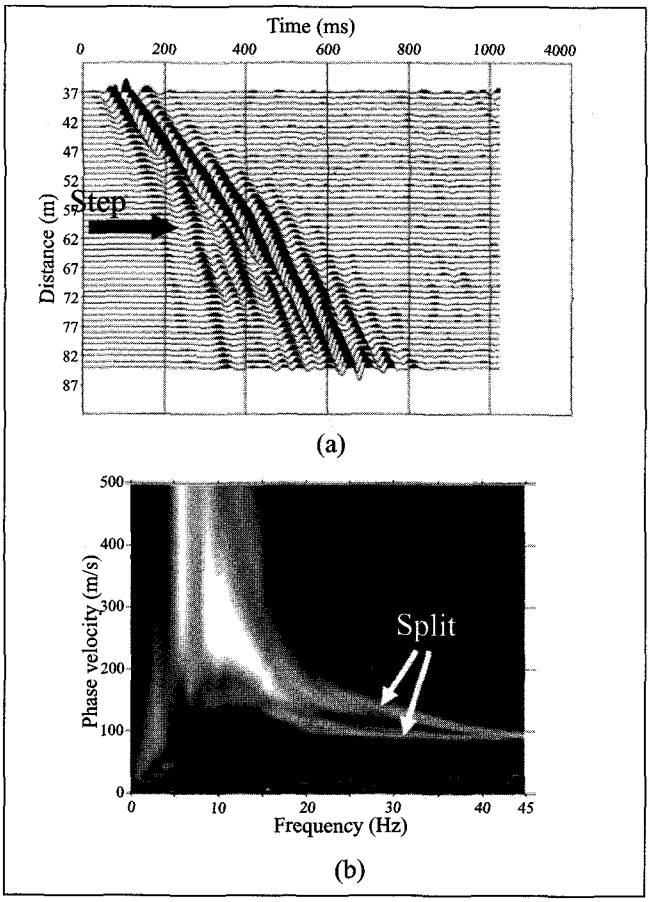

Fig. 7. Shot gathers (a) of 35.8 m shot and its c–f image (b).

characteristic phase differences at each CMP location, and can be handled in the same way as shot gathers in the phase-velocity analysis. We have named it the CMPCC gather.

5. The MASW method is applied to the CMPCC gathers, to calculate phase velocities. First, each trace is transformed into the frequency domain using the Fast Fourier Transform (FFT). Then, the frequency-domain data is integrated over the spacing with respect to apparent velocities. In this way, the CMPCC gathers in distance-time space can be transformed into *c-f* space directly.
6. Phase velocities are determined from the maximum amplitude at each frequency.

NUMERICAL EXAMPLE

A numerical test was performed in order to evaluate the proposed method. Figures 5 and 6 show a velocity model used in the test, and the source-receiver geometry, respectively. The model is a three-layer structure having a step discontinuity at the distance of 60 m. A stress-velocity, staggered grid, 2D finite-difference method (Levander, 1988) was used for waveform calculation. Figures 7a and 7b show a shot gather and its *c–f* image, for a shot located at 35.8 m. The apparent velocity of the time-domain waveforms changes abruptly at the 60 m point, corresponding to the step. A phase-velocity curve in the *c–f* image splits into two curves in the frequency range between 15 and 40 Hz. The CMPCC analysis was applied to the numerical data. All shot gathers were used in the analysis. Figure 8a and 8b show resultant CMPCC gathers in which common-mid-point cross-correlations are ordered with respect to their spacing. We can see that the obvious change of apparent velocity is not apparent in the time-domain waveform displays of the CMPCC gathers. In each of the *c–f* images, the energy is concentrated in one phase velocity curve.

A non-linear least squares method (Xia et al., 1999) was applied to the dispersion curves to reconstruct the 2D S-wave velocity profile. An initial model was generated by a simple wavelength-depth conversion. The number of layers was fixed at 15, and only S-wave velocities were changed throughout the inversion. The inverted S-wave velocity profile obtained by CMPCC analysis (Figure 9a) shows better spatial resolution when compared with that obtained by the conventional MASW analysis (Figure 9b). The step discontinuity at the middle of the section is more clearly imaged by the CMPCC analysis.

APPLICATION TO FIELD DATA

The CMPCC analysis was applied to the field surface-wave data shown in Figure 1. The survey site was located in Hokkaido Island, Japan. The purpose of the survey was to detect a buried channel beneath a flood plain. A 10 kg sledgehammer was used as a source. The source interval was 4 m. Forty-eight geophones (4.5 Hz) were deployed at 1 m intervals. The nearest source-to-receiver offset was 1 m. Fifty-two shot gathers were recorded with an OYO-DAS1 seismograph.

Figures 10a and 10b show the resultant CMPCC gathers and their *c–f* images. The CMPs are at 173 m (Figure 10a) and 201 m (Figure 10b), in the first half and the latter half of the spread, respectively. Changes in surface-wave velocity are not apparent in the time-domain waveform displays of the CMPCC gathers. In each of the *c–f* images, it is obvious that energy is concentrated into one phase velocity curve.

A 2D S-wave velocity model was constructed using the same method described above. The number of layers was again fixed at 15. Figures 11a-11c show the S-wave velocity models obtained from MASW (Figure 11a) and CMPCC (Figure 11b), and the geological interpretation (Figure 11c). N-value curves obtained from an automatic ram-sounding are superimposed on the resulting sections. The 2D S-wave velocity structure derived by CMPCC analysis coincides well with the N-value curves.

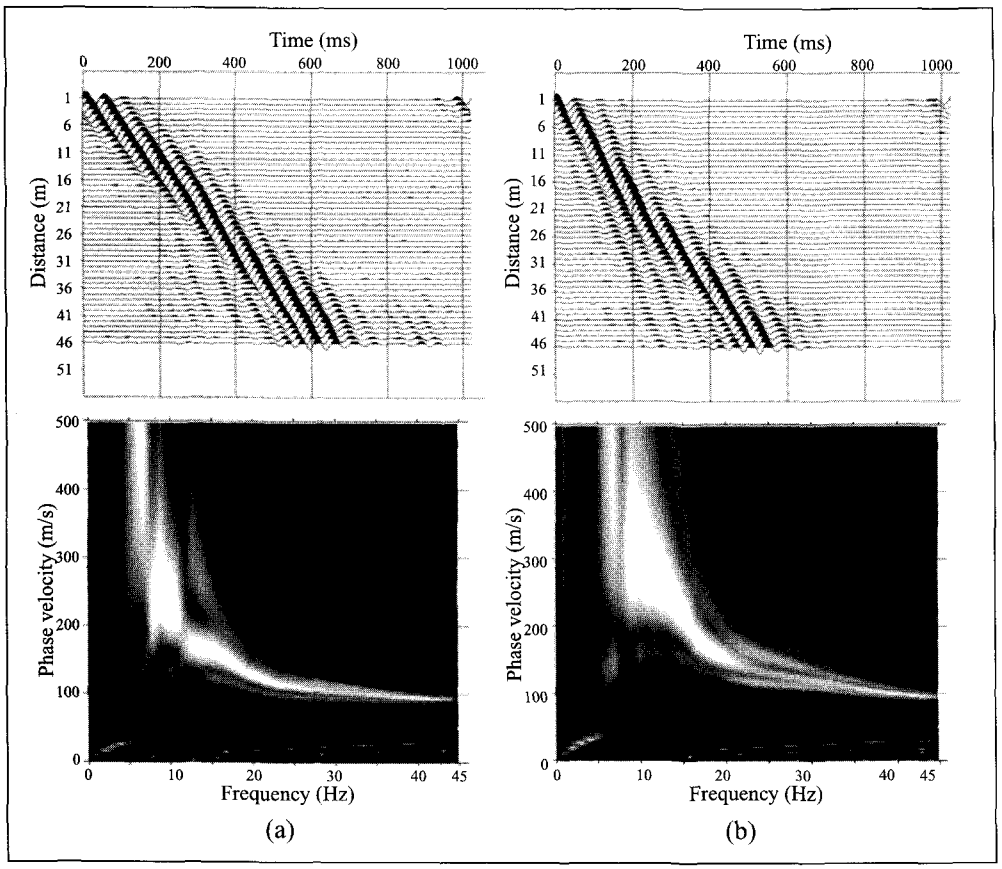

Fig. 8. CMPCC gathers obtained through CMPCC analysis (top), and their *c–f* images (bottom). The data correspond to two lateral distances: 50.8 m (a) and 70.8 m (b). The velocity structure changes laterally between those distances.

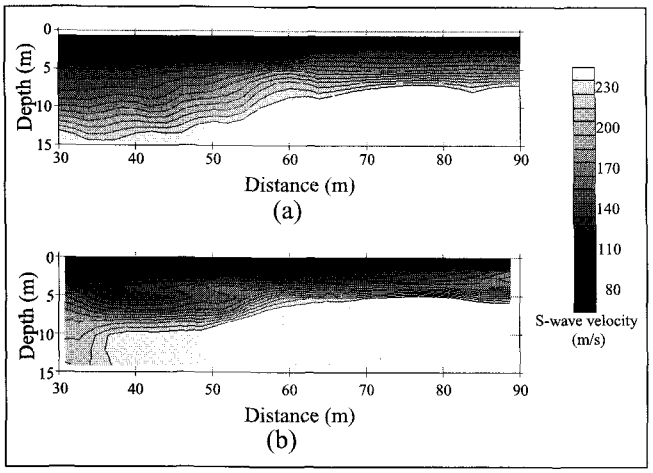

Fig. 9. S-wave cross-section obtained from (a) conventional MASW processing and (b) CMPCC processing.

Variations between the N-value curves along the line suggest that the velocity structure should change horizontally between S2 (120 m) and S1 (200 m). In the S-wave velocity section defined by the surface-wave method, the thickness of the low-velocity layer (alluvial sediments) changes at the 175 m mark. Based on this interpretation of the S-wave velocity structure obtained using the surface-wave method, together with the penetrometer logs, we can conclude that there is a buried channel filled with alluvium sediments, extending beyond the distance of 175 m (Figure 11c).

CONCLUSIONS

One of the notable features of the CMPCC analysis is that it does not require any summation or averaging of phase differences. The reason is that the CMPCC analysis processes the multi-channel and multi-shot waveform data into the cross-correlations. The conventional SASW method determines phase velocities from differently spaced cross-correlations separately. The SASW method cannot determine high-frequency phase velocities from large-spacing cross-correlations because of spatial aliasing. Therefore, SASW uses only a limited part of whole-waveform data. MASW analysis is better than SASW because MASW can determine phase velocities precisely using whole waveform data (McMechan and Yedlin, 1981; Park et al., 1999a, 1999b). CMPCC analysis is a further extension of MASW that enables us to determine phase velocities from multi-shot data directly, by using CMPCC gathers. The method not only improves the accuracy and resolution of the MASW method, but it also enables the SASW method to perform a pseudo multi-channel analysis in order to distinguish a fundamental mode from higher modes visually.

ACKNOWLEDGEMENTS

The authors thank the Obihiro Development and Construction Department of the Hokkaido Regional Development Bureau, and Japan Institute of Construction Engineering for their support for fieldwork and the permission to publish the data. The manuscript has been improved by the helpful comments and suggestions of Dr. O. Nishizawa, T. Inazaki, and an anonymous reviewer.

REFERENCES

Hayashi, K., 2001, Surface wave propagation in two-dimensional models and its application to near-surface S-wave velocity delineation: *Proceedings of the 5th SEGJ international symposium*, 385–392.

Levander, A.R., 1988, Fourth-order finite-difference P-SV seismograms: *Geophysics*, **53**, 1425–1436.

McMechan, G.A., and Yedlin, M.J., 1981, Analysis of dispersive waves by wave field transformation: *Geophysics*, **46**, 869–874.

Miller, R.D., Xia, J., Park, C.B., and Ivanov, J.M., 1999, Multichannel analysis of surface waves to map bedrock: *The Leading Edge*, **18**, 1392–1396.

Nazarian, S., Stokoe, K.H., and Hudson, W.R., 1983, Use of spectral analysis of surface waves method for determination of moduli and thickness of pavement system: *Transport. Res. Record*, **930**, 38–45.

Park, C.B., Miller, R.D., and Xia, J., 1999a, Multimodal analysis of high frequency surface waves: *Proceedings of the symposium on the application of geophysics to engineering and environmental problems* '99, 115–121.

Park, C.B., Miller, R.D., and Xia, J., 1999b, Multichannel analysis of surface waves: *Geophysics*, **64**, 800–808.

Xia, J., Miller, R.D., and Park, C.B., 1999, Configuration of near surface shear wave velocity by inverting surface wave: *Proceedings of the symposium on the application of geophysics to engineering and environmental problems* '99, 95–104.

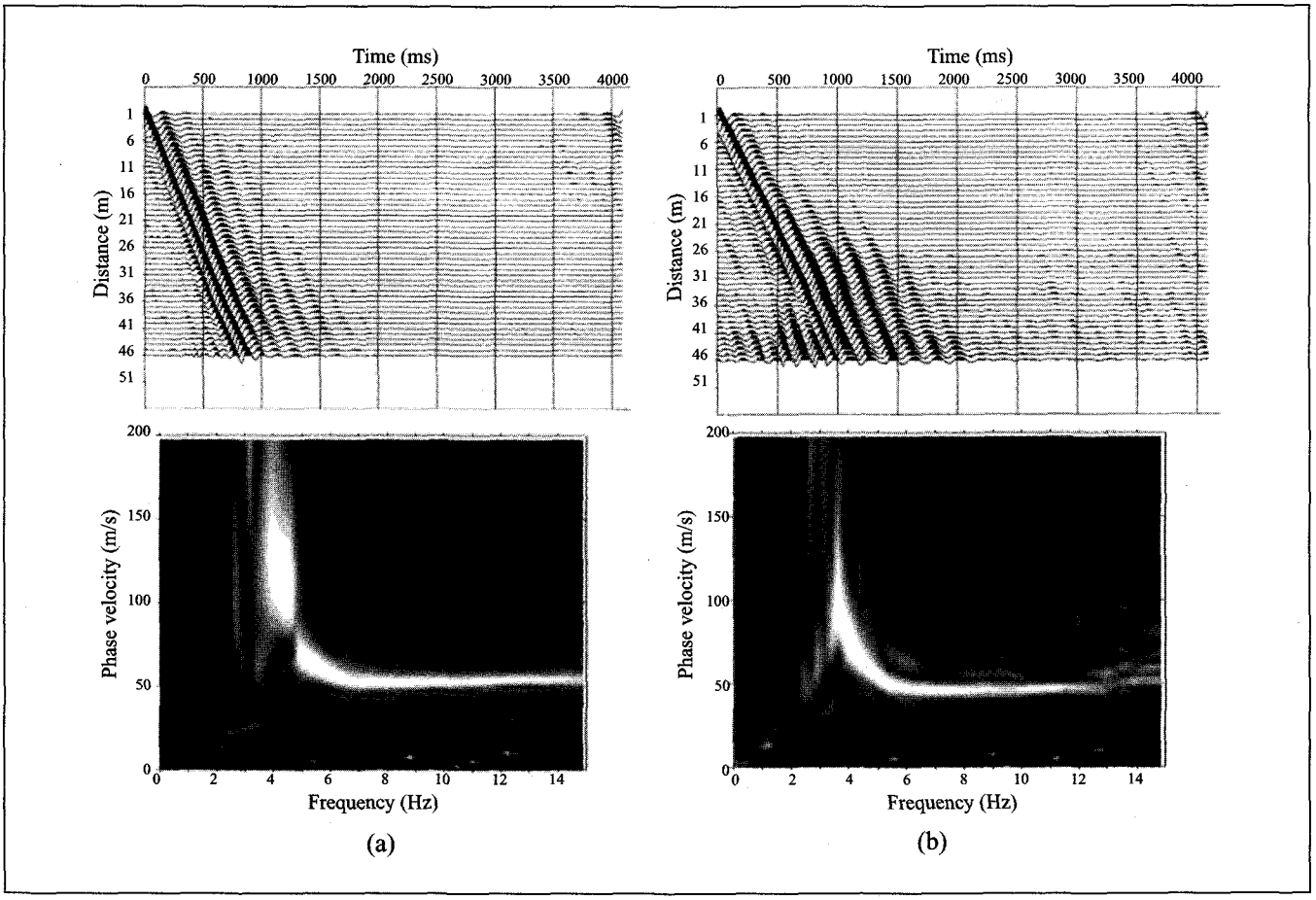

Fig. 10. Result of CMPCC analysis of the data shown in Figure 1. CMPCC gathers (top) and their *c–f* images (bottom). CMP distances are 173 m (a) and 201 m (b).

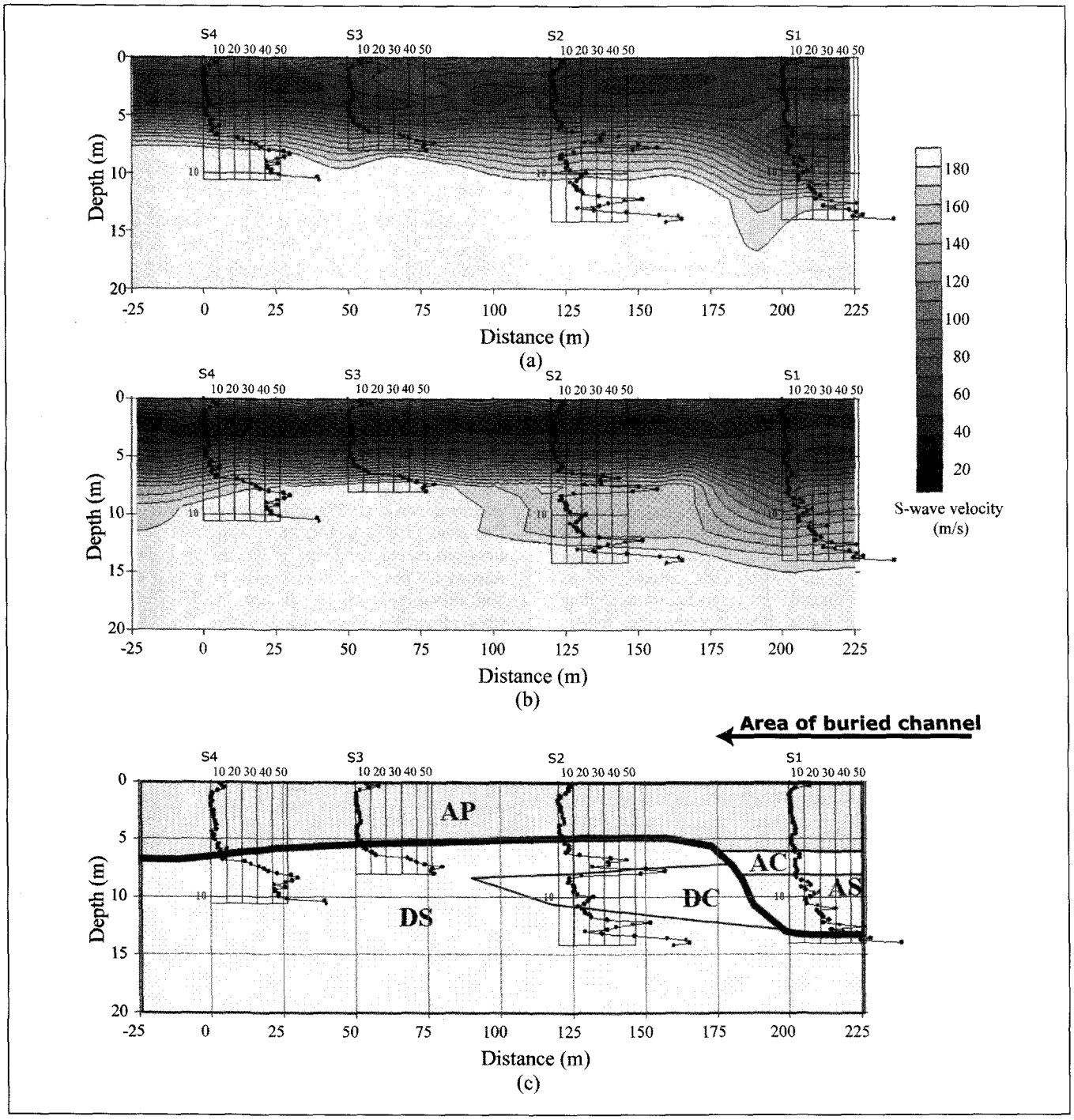

Fig. 11. S-wave velocity structure defined by (a) the conventional MASW method and (b) the CMPCC method, together with a geological section (c) estimated from N-values obtained by an automatic ram-sounding. The surface geology consists of peat alluvium (AP), clay alluvium (AC), sand alluvium (AS), clay weathered layer (DC), and sand weathered layer (DS).